Journal of Alloys and Compounds 513 (2012) 125–129

Contents lists available at SciVerse ScienceDirect

Journal of Alloys and Compounds

journal homepage: www.elsevier.com/locate/jallcom

Porous ZnO platelets via controlled thermal decomposition of zinc glycerolate

Hailong Dong, Claus Feldmann*

Institut für Anorganische Chemie, Karlsruhe Institute of Technology (KIT), Engesserstraße 15, D-76131 Karlsruhe, Germany

ARTICLE INFO

Article history:
Received 17 March 2011
Received in revised form
27 September 2011
Accepted 3 October 2011
Available online 17 October 2011

Keywords:
Nanomaterial
Zinc oxide
Zinc glycerolate
Thermal decomposition
Platelet
Porous

ABSTRACT

Zinc glycerolate, Zn(gly), is prepared via a polyol-mediated synthesis with platelet-like morphology. These platelets exhibit diameters of 10–15 μm and a thickness of 100–300 nm. Via controlled thermal decomposition at 500–600 °C as-prepared Zn(gly) can be reacted to ZnO with the platelet-like morphology maintained. The loss of the spacious (gly)-ligand is accompanied by a granulated sub-structure of the ZnO platelets that now exhibit lots of pores. By controlled thermal decomposition, moreover, the porosity of the granulated ZnO platelets can be adjusted with specific surfaces of 5–18 $m^2 g^{-1}$ and pore volumes of 25–230 $mm^3 g^{-1}$. Particle size, morphology and composition of Zn(gly) and ZnO are validated by electron microscopy, X-ray powder diffraction, infrared spectroscopy, thermogravimetry and nitrogen sorption analysis.

1. Introduction

Nanostructured zinc oxide is highly relevant to applications such as UV-protection and sunblocking [1], catalysis/photocatalysis [2], dye-sensitized solar cells [3] and transparent oxide conductors [4]. Its synthesis has been performed by various gas- and liquid-phase methods that are summarized in several recent reviews [5–8]. In fact, nanostructured ZnO can be precisely adjusted in size all over the complete nanoscale range (i.e. 1–100 nm) by selecting a suitable method of preparation. Due to the hexagonal symmetry of the ZnO lattice [9], most often rod-like particles and structures are gained [10,11]. Non-isotropic morphologies such as platelets are less often observed although they could be highly relevant for thin-films that exhibit an oriented reflection of light or a directed electrical conductivity. Such platelet-like ZnO has been yet gained by physicochemical techniques such as electrochemical deposition [12], radio-frequency sputtering [13], ultrasonic spray pyrolysis [14] as well as by applying long-chained amines/carboxylates for a structure-directed growth in solution [15–17].

Amongst the methods to prepare high-quality ZnO nanoparticles, the so-called polyol method is widely applied, too [18,19]. Typically, zinc acetate dihydrate is hydrolyzed by heating in a multivalent, high-boiling alcohol – named “polyol” – such as 1,4-butandiol or diethylene glycol. Nowadays, the polyol method represents a standard synthesis with various compounds that are accessible as monodisperse, non-agglomerated and crystalline nanoparticles [20,21]. Although the polyol method is quite beneficial with concern to the formation of ZnO nanoparticles, it is well-known that the synthesis fails if glycerol is applied as the polyol. In such a case large crystals of zinc glycerolate (Zn(gly)) are obtained as the only product [22]. On the nanoscale, Zn(gly) has been just obtained with spherical particles via microemulsion approaches [23–25].

In this study, Zn(gly) platelets were prepared via the polyol approach. By a suited thermal treatment the as-prepared Zn(gly) was decomposed to ZnO with the platelet-like morphology still remaining. Based on the concrete conditions of thermal decomposition, the porosity and surface of the ZnO platelets can be adjusted. Such porous ZnO platelets are here first observed.

2. Experimental

2.1. Synthesis of zinc glycerolate

As a typical recipe, 2.00 g zinc acetate dihydrate (9.1 mmol, 99%, Acros Organics), 50 ml glycerol (99+ %, Acros Organics) and 1 ml of distilled water were added into a 100 ml flask under Argon flow. The resulting solution was heated to 160 °C and refluxed for 1 h under moderate stirring. After natural cooling to room temperature, the colorless precipitate was collected via centrifugation at 25,000 rpm for 20 min. Thereafter the solid residue was washed three times by resuspension in and centrifugation from ethanol. Finally, Zn(gly) was dried at 80 °C for 60 min.

2.2. Thermal decomposition of as-prepared Zn(gly)

50 mg of as-prepared Zn(gly) was heated with different thermal procedures as listed in Table 1. Heating was performed in tube furnaces (HTM Reetz LOBA 1200)

---

* Corresponding author. Tel.: +49 721608 42855; fax: +49 721608 44892.
E-mail address: claus.feldmann@kit.edu (C. Feldmann).

0925-8388/$ – see front matter © 2011 Elsevier B.V. All rights reserved.
doi:10.1016/j.jallcom.2011.10.004

Table 1
Experimental conditions of thermal decomposition of as-prepared Zn(gly) platelets and resulting specific surface (BET) and pore volume (BJH) of ZnO.

Sample	Heating rate, °C h^{-1}	Max. temperature, °C	Duration at T_{max}, min	Specific surface (BET), $m^2\,g^{-1}$	Pore volume (BJH), $mm^3\,g^{-1}$
Zn(gly)	–	–	–	2.2	14.9
ZnO (fast)	∞[a]	600	30	5.2	29.1
ZnO (medium)	60	500	30	17.6	232.2
ZnO (slow)	10 (20 → 300 °C)5 (300 → 500 °C)	500	30	5.9	24.6

[a] Sample was introduced into the hot oven at 600 °C and removed after 30 min.

and performed via programmed temperature control. All powder samples were deposited in alumina crucibles.

2.3. Analytical characterization

The morphology of Zn(gly) and ZnO was characterized by a Supra 40 VP scanning electron microscope (SEM) from Zeiss. Fourier-transformed infrared spectra (FT-IR) of the samples were recorded applying KBr tablets by a Vertex 70 FT-IR spectrometer from Bruker Optics. Every tablet contained 1.5 mg of the sample and 300 mg of KBr (FT-IR grade). Crystallinity and purity of powder samples were validated based on X-ray diffraction pattern that were recorded on a Stoe Stadi-P X-ray diffractometer with Ge-monochromatized Cu-Kα radiation (XRD, λ = 154 pm). Thermogravimetry (TG) was performed with a STA 409C instrument from Netzsch. The Brunauer–Emmett–Teller (BET) surface of the samples was determined from nitrogen sorption measurements using a Belsorp Mini II apparatus from BEL.

3. Result and discussion

3.1. Synthesis and characterization of Zn(gly) platelets

Zn(gly) platelets were obtained via the polyol-mediated synthesis utilizing a solution of $Zn(Ac)_2 \cdot 2H_2O$ in glycerol (gly) that was heated to 160 °C. At about 120 °C the solution became turbid which indicates the precipitation of solid Zn(gly). When naturally cooled to room temperature the resulting milky suspension was centrifuged. The colorless remnant was thrice resuspended in and centrifuged from ethanol in order to remove excess glycerol and all remaining salts. Finally, the colorless residue was dried (60 min, 80 °C) and thereafter investigated based on state-of-the-art analytical tools with regard to particle size and morphology, chemical composition and crystallinity.

Scanning electron microscopy (SEM) evidences the presence of platelet-like particles with diameters of 10–15 μm and a thickness of about 100–300 nm (Fig. 1). X-ray powder diffraction pattern (XRD) confirm the chemical composition of the as-prepared platelets as Zn(gly) (Fig. 2). All Bragg peaks observed are well in agreement with literature data [23]. Infrared spectra (FT-IR) of the as-prepared Zn(gly) platelets are also in complete agreement with reference data of bulk-Zn(gly) [26]. Note that the splitting of vibrational bands as observed for Zn(gly) originates from the reduced site symmetry of the solid lattice as compared to the non-bound molecule in the liquid phase. When comparing to pure glycerol as a reference, the strong bands at 2700–2400, 2050–1900 and 1500–1350 cm^{-1} look somewhat unusual. However, these bands are observed in all available reference spectra with similar intensity and shape and were ascribed to O–H···O bending modes that are not specified in detail [22,23].

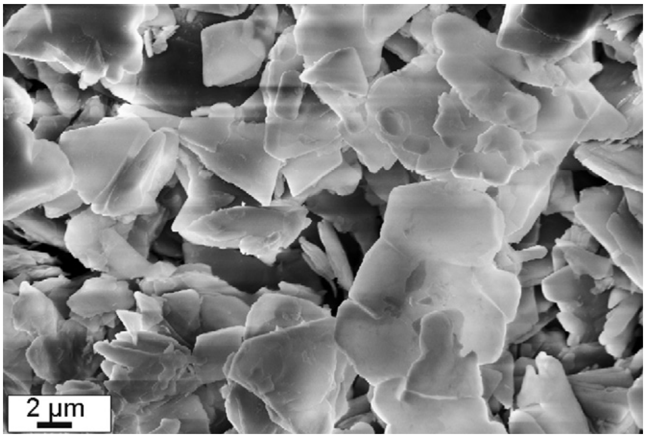

Fig. 1. Scanning electron microscopy (SEM) of as-prepared Zn(gly) platelets.

Thermogravimetry (TG) elucidates the thermal decomposition of the as-prepared Zn(gly) platelets (Fig. 3). Accordingly, decomposition occurred with a single massive weight-loss of 47% that starts at 310 °C and that is finished at 470 °C. This value matches exactly with the expectation (48%) when assuming a thermal decomposition of Zn(gly) in air under formation of ZnO. Based on the TG analysis and a temperature of 470 °C required for complete decomposition, larger quantities of as-prepared Zn(gly) were used for controlled decomposition at 500–600 °C inside of a tube furnace. The white powder obtained as the thermal remnant was again investigated by XRD (Fig. 4). Accordingly, pure ZnO was obtained by thermal decomposition of Zn(gly).

3.2. Synthesis and characterization of porous ZnO platelets

Since the availability of ZnO with platelet-like morphology is limited till now [12–17], and while such a material with non-isotropic morphology could be highly interesting with concern

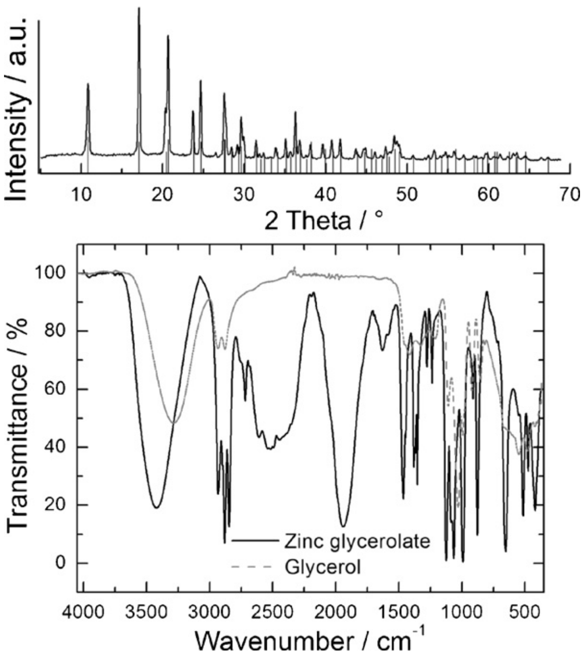

Fig. 2. XRD powder pattern and FT-IR spectra of as-prepared Zn(gly) platelets. XRD powder pattern of bulk-Zn(gly) (ICDD No. 23-1975) and FT-IR spectra and pure glycerol as references.

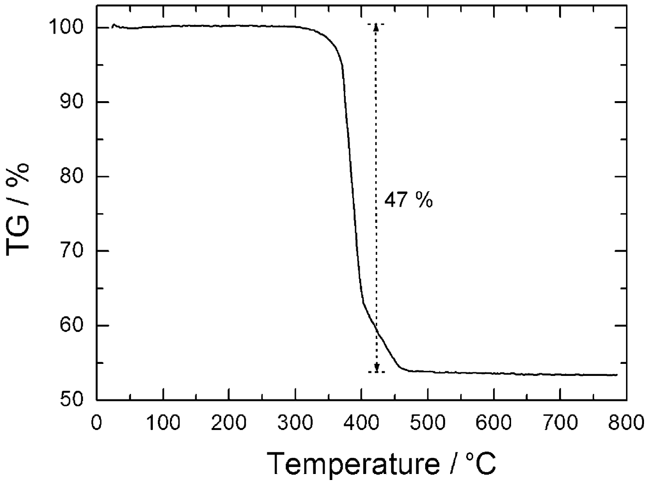

Fig. 3. Thermogravimetry of as-prepared Zn(gly) platelets (total weight: 20.6 mg; heating rate: 20 °C min^{-1}).

to its catalytical, optical and electronical properties, the question arises whether thermal decomposition of platelet-like Zn(gly) can be performed while maintaining its morphology. To this concern, as-prepared Zn(gly) was decomposed with fast, moderate and slow heating rates inside of a tube furnace. The detailed conditions of heating, including heating rate, temperature and duration of heating are listed in Table 1.

According to SEM images the morphology of the resulting ZnO particles significantly depends on the conditions of heating (Table 1 and Figs. 5–7). In the case of fast heating, the morphology of the initial Zn(gly) platelets obviously remains intact and results in ZnO with a still similar platelet-like morphology, 10–15 μm in diameter and a thickness of about 100–300 nm. Thus, the platelets exhibit a large aspect ratio of ~100. In contrast to Zn(gly), the ZnO platelets now exhibit a granulated morphology consisting of aggregated particles of 200–300 nm in size (Fig. 5). The massive glycerolate-driven weight-loss, moreover, causes the formation of lots of pores inside of the granulated structure. These pores exhibit diameters of up to 100 nm. While performing nitrogen sorption, Brunauer–Emmett–Teller (BET) and Barret–Joyner–Halenda (BJH) analysis result in a specific surface of 5.2 m^2 g^{-1} and a pore volume of 29.1 mm^3 g^{-1}. In fact, these values are only doubled in comparison to the as-prepared Zn(gly) (Table 1). With moderate heating the platelet-like morphology remains intact, too (Fig. 6). Again the platelets exhibit a granulated structure with lots of pores. In contrast to the findings for fast heating, the granulated structure is however established by much smaller particles that exhibit diameters of only about 10–30 nm. This ten times smaller granulated sub-structure is accompanied by a significantly increased specific surface and pore volume. Thus, values of 17.6 m^2 g^{-1} (BET) and 232.2 mm^3 g^{-1} (BJH) were obtained now (Table 1).

While further reducing the heating rate, an even increased specific surface and pore volume could have been expected. Slow heating, however, only led to very small specific surfaces (5.9 m^2 g^{-1}) and pore volumes (24.6 mm^3 g^{-1}) (Table 1). Electron microscopy furthermore indicates that the platelet-like morphology is not preserved here (Fig. 7). In contrast, irregularly agglomerated, more or less spherical nanoparticles with diameters of 100–200 nm are obtained.

In sum, the decomposition of Zn(gly) – as expected – leads to the formation of ZnO. If the decomposition is fast, the platelet-like morphology of the starting material remains intact for the product, too. The dramatic volume reduction due to the loss of the spacious (gly)-ligand is accompanied by pore formation and platelets exhibiting a granulated sub-structure. Since the decomposition of Zn(gly) is more controlled at slower heating rates, smaller grains and a higher

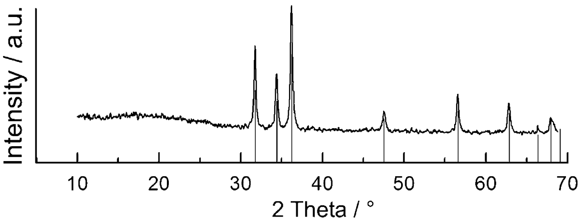

Fig. 4. XRD powder pattern of ZnO platelets with bulk-ZnO as a reference (ICDD 34-1451).

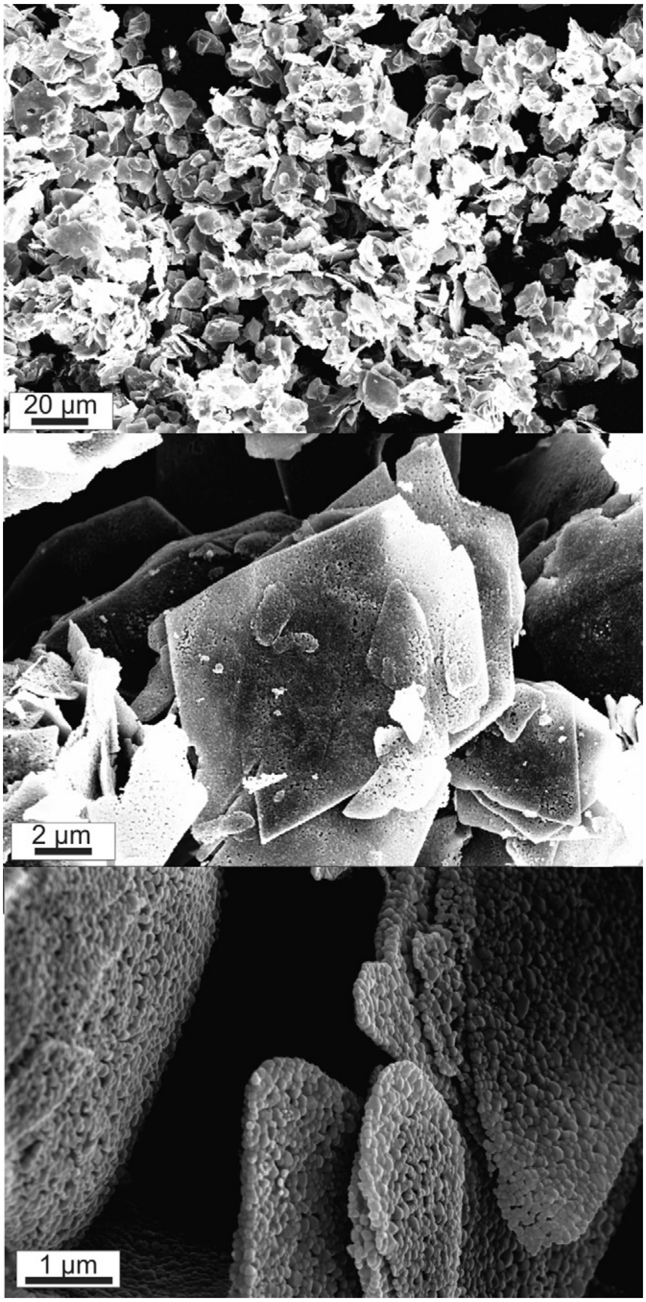

Fig. 5. Scanning electron microscopy at different level of magnification of porous ZnO platelets obtained via fast thermal decomposition of Zn(gly) (A: large scale overview; B: top-view of porous platelet with high resolution; C: side-view of porous platelet with high resolution).

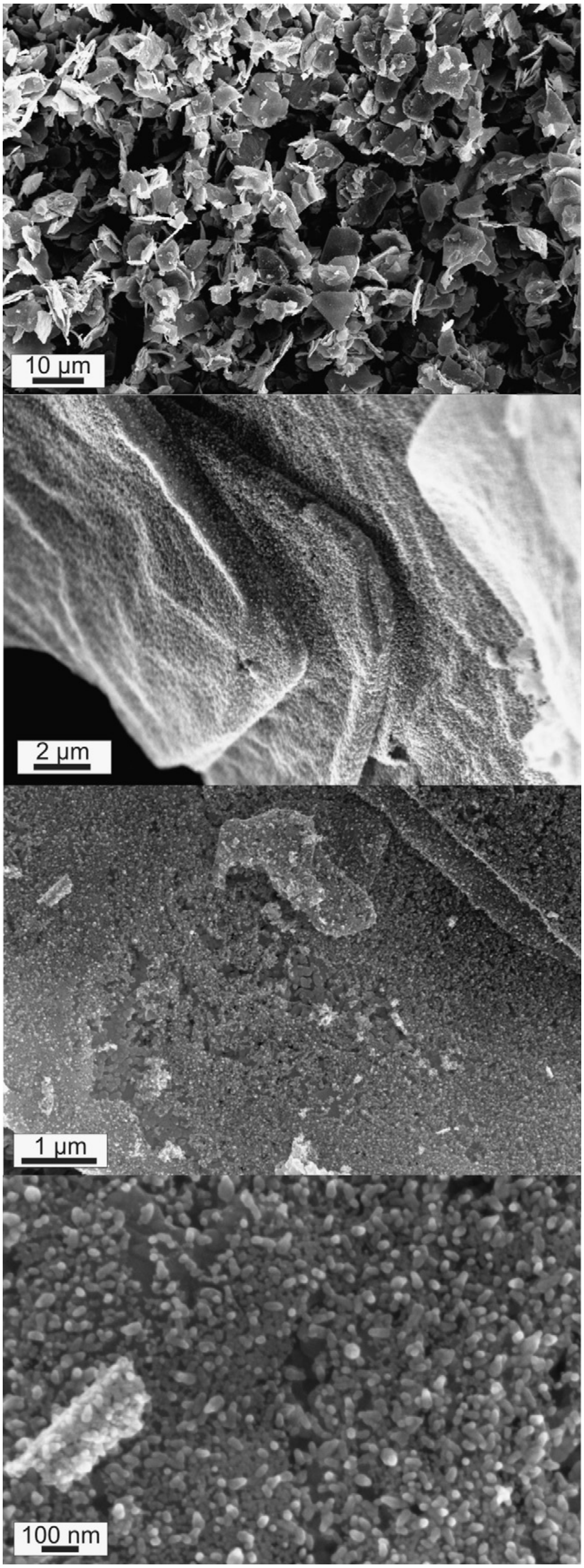

Fig. 6. Scanning electron microscopy at different level of magnification of porous ZnO platelets obtained via moderate thermal decomposition of Zn(gly) (A: large scale overview; B: side-view of porous platelet with high resolution; C, D: top-view of porous platelet with high resolution).

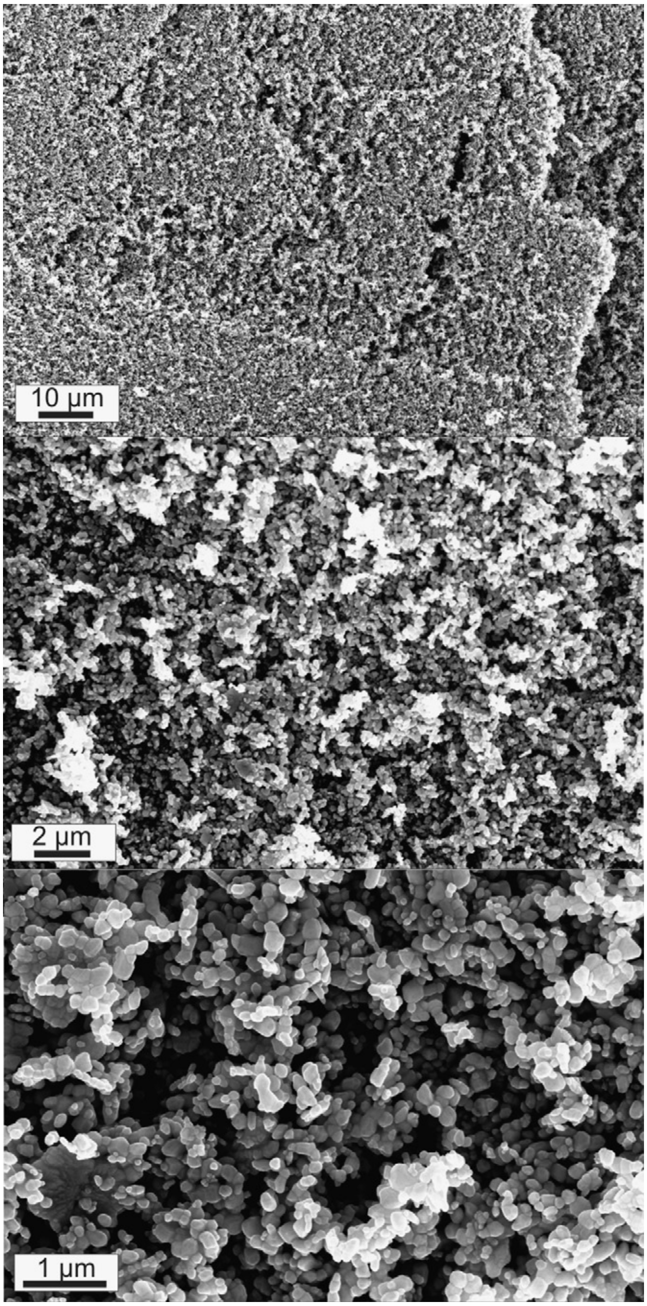

Fig. 7. Scanning electron microscopy at different level of magnification of spherical ZnO particles obtained via slow thermal decomposition of Zn(gly).

specific surface and pore volume are obtained for the granulated ZnO platelets in the latter case. Thus, moderate heating leads to a higher porosity than fast heating. On the other hand, a certain sintering even at temperatures as low as 400 °C has to be taken into account [27]. Sintering will be the faster, the smaller the ZnO grains are. If – via slow heating – the ZnO grains become very small, the prolonged time at elevated temperatures (>400 °C) favors a certain sintering of the nanostructured ZnO. As a result, the loss of the platelet-like morphology and the formation of spherical and dense ZnO nanoparticles are observed. Via advanced heating processes it might be nevertheless possible to increase the specific surface and the pore volume even further. Moreover, other porous oxides might be available based on a controlled decomposition of metal glycerolates.

4. Conclusions

Thermal decomposition of zinc glycerolate, Zn(gly), gives access to ZnO at temperatures of 500–600 °C. Most interestingly the platelet-like morphology of the as-prepared Zn(gly) can be preserved during the formation of ZnO that still exhibits a platelet-like morphology with diameters of 10–15 μm and a thickness of 100–300 nm. Controlled decomposition of Zn(gly), moreover, allows adjusting a certain porosity of the now granulated ZnO platelets with specific surfaces (BET) of 5–18 $m^2 g^{-1}$ and pore volumes (BJH) of 25–230 $mm^3 g^{-1}$. Since an initial growth of platelet-like ZnO is often not observed, thermal decomposition of Zn(gly) could be a useful alternative. Such porous ZnO platelets with a large aspect ratio (∼100) can be relevant for applications such as UV-protection, sunblocking or catalysis.

Acknowledgement

The authors are grateful to the Center for Functional Nanostructures (CFN) of the Deutsche Forschungsgemeinschaft (DFG) at the Karlsruhe Institute of Technology (KIT) for financial support.

References

[1] S. Schnittger, M. Sinha, MRS Bull. 32 (2007) 760.
[2] H. Goesmann, C. Feldmann, Angew. Chem. Int. Ed. 49 (2010) 1362.
[3] Q. Zhang, C.S. Dandeneau, X. Zhou, G. Cao, Adv. Mater. 21 (2009) 4087.
[4] T. Minami, Semicond. Sci. Technol. 20 (2005) 35.
[5] F. Weiss, M. Audier, A. Bartasyte, D. Bellet, C. Girardot, C. Jimenez, J. Kreisel, S. Pignard, M. Salaun, C. Ternon, Pure Appl. Chem. 81 (2009) 1523.
[6] W. Gao, Z. Li, Int. J. Nanotechnol. 6 (2009) 245.
[7] E. McGlynn, M.O. Henry, J.P. Mosnier, in: A.V. Narlikar, B.Y. Yu (Eds.), The Oxford Handbook of Nanoscience and Technology, vol. 2, Oxford University Press, New York, 2010, p. 523.
[8] D. Lincot, MRS Bull. 35 (2010) 778.
[9] S.C. Abrahams, J.L. Bernstein, Acta Crystallogr. B 25 (1969) 1233.
[10] C. Klingshirn, Phys. Status Solidi B 244 (2007) 3027.
[11] C. Pacholski, A. Kornowski, H. Weller, Angew. Chem. Int. Ed. 41 (2002) 1188.
[12] X. Lü, X. Zou, J. Cheng, G. Yang, C. Wei, Z. Sun, J. Feng, Y. Yang, G. Teng, X. Meng, Adv. Mater. Res. 123–125 (2010) 703.
[13] J.Y. Ye, Z.Y. Huang, C. Min, S.R. Pan, D.J. Chen, Biomed. Mater. 4 (2009) 0550041.
[14] M.T. Htay, Y. Hashimoto, K. Ito, Jpn. J. Appl. Phys. 46 (2007) 440.
[15] P.D. Burton, E.J. Peterson, T.J. Boyle, A.K. Datye, Catal. Lett. 139 (2010) 26.
[16] G. Han, A. Shibukawa, M. Okada, Y. Neo, T. Aoki, H. Mimura, J. Vac. Sci. Technol. B 28 (2010) C2C16.
[17] H. Tang, J.C. Chang, Y. Shan, S.T. Lee, J. Phys. Chem. B 112 (2008) 4016.
[18] D. Jezequel, J. Guenot, N. Jouini, F. Fievet, J. Mater. Res. 10 (1994) 77.
[19] J. Merikhi, C. Feldmann, J. Colloid Interface Sci. 223 (2000) 229.
[20] P. Toneguzzo, G. Viau, O. Acher, F. Guillet, E. Bruneton, F. Fievet-Vincent, F. Fievet, J. Mater. Sci. 35 (2000) 3767.
[21] C. Feldmann, Adv. Funct. Mater. 13 (2003) 101.
[22] E.W. Radoslovich, M. Raupach, P.G. Slade, R.M. Taylor, Aust. J. Chem. 23 (1970) 1963.
[23] J. Das, D. Khushalani, J. Phys. Chem. C 114 (2010) 2544.
[24] O.A. Yildirim, C. Durucan, J. Alloys Compd. 506 (2010) 944.
[25] R. Moleski, E. Leontidis, F. Krumeich, J. Colloid Interface Sci. 301 (2006) 246.
[26] T.W. Hambley, M.R. Snow, Aust. J. Chem. 36 (1983) 1249.
[27] X. Su, Z. Zhang, M. Zhu, Appl. Phys. Lett. 88 (2006) 061913.